

BrainVis: Exploring the Bridge between Brain and Visual Signals via Image Reconstruction

Honghao Fu^{1, 2}, Zhiqi Shen², Jing Jih Chin², Hao Wang^{1*}

¹The Hong Kong University of Science and Technology (Guangzhou), China

²Nanyang Technological University, Singapore

Abstract

Analyzing and reconstructing visual stimuli from brain signals effectively advances the understanding of human visual system. However, the EEG signals are complex and contain significant noise. This leads to substantial limitations in existing works of visual stimuli reconstruction from EEG, such as difficulties in aligning EEG embeddings with the fine-grained semantic information and a heavy reliance on additional large self-collected dataset for training. To address these challenges, we propose a novel approach called BrainVis. Firstly, we divide the EEG signals into various units and apply a self-supervised approach on them to obtain EEG time-domain features, in an attempt to ease the training difficulty. Additionally, we also propose to utilize the frequency-domain features to enhance the EEG representations. Then, we simultaneously align EEG time-frequency embeddings with the interpolation of the coarse and fine-grained semantics in the CLIP space, to highlight the primary visual components and reduce the cross-modal alignment difficulty. Finally, we adopt the cascaded diffusion models to reconstruct images. Using only 10% training data of the previous work, our proposed BrainVis outperforms state of the arts in both semantic fidelity reconstruction and generation quality. The code is available at <https://github.com/RomGai/BrainVis>.

1 Introduction

Advancements in deep learning have markedly enhanced the ability to decode complex neural signals (Alzahab et al. 2021), laying the groundwork for studies investigating neural responses to external stimuli (Lin, Sprague, and Singh 2022; Lee et al. 2023; Banaszekiewicz et al. 2021). This body of research extends to exploring the nexus of neural signals with sensory perceptions such as auditory, olfactory, and visual stimuli (Geirnaert et al. 2021; Wu et al. 2023; Spampinato et al. 2017). Particularly, investigating how the brain processes visual information is paramount for advancing our comprehension of the visual functions of the human brain. Nevertheless, deciphering the brain’s visual system is complicated by the extensive involvement of neurons (Hutmacher 2019).

In response, recent investigations have enlisted deep neural networks for the extraction of visual information from neural signals, reconstructing images semantically related to these

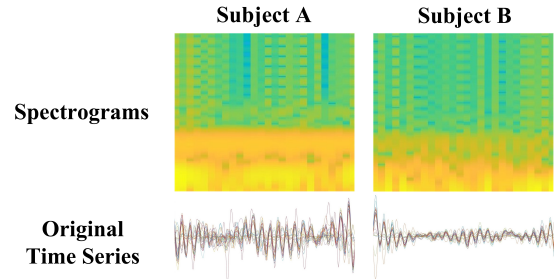


Figure 1: Time series and spectrograms of EEG signals from two subjects, both derived from the same visual stimulus.

signals to explore the visual semantic components contained in neural signals (Fang, Qi, and Pan 2020; Lin, Sprague, and Singh 2022; Takagi and Nishimoto 2023a; Rombach et al. 2022; Kavasidis et al. 2017; Tirupattur et al. 2018; Singh et al. 2023). Electroencephalography (EEG), capturing general brain activity via scalp electrodes to generate multi-channel 2D temporal sequences (Spampinato et al. 2017), stands out for its affordability and simplicity in processing (Khosla, Khandnor, and Chand 2020). Despite these benefits, EEG’s limited spatial resolution, the challenge of accurately localizing brain regions, and susceptibility to extraneous noise make reconstructing images from EEG signals a formidable task (Lai et al. 2018).

Previous methods integrating Long Short-Term Memory (LSTM) models and Generative Adversarial Networks (GAN) have faced limitations due to the scarcity of training data for GANs, resulting in subpar semantic accuracy and image quality (Kavasidis et al. 2017; Tirupattur et al. 2018; Singh et al. 2023). A novel approach employing Masked Autoencoders (MAE) (He et al. 2022) and latent diffusion model (LDM) (Rombach et al. 2022) showed promise with improved reconstruction outcomes. However, this strategy encounters its own set of challenges: (1) poor feature embedding capability, relying on extra datasets for better representation; (2) neglecting frequency features as shown in Fig. 1, which possess unique characteristics divergent from those of the time domain (Al-Fahoum and Al-Fraihat 2014); (3) only coarse-grained category reconstruction, missing fine-grained semantic details.

To overcome these limitations, we propose **BrainVis**, a

*Corresponding Author

novel pipeline for EEG-based image reconstruction. It comprises three components: (1) EEG encoder, including self-supervised latent masked modeling and frequency features to enhance EEG representations; (2) Semantic interpolation cross-modal alignment, aligning EEG embeddings with coarse and fine-grained semantics in the CLIP (Radford et al. 2021) space to highlight primary visual components and reduce alignment difficulty; (3) Cascaded diffusion models, using aligned fine-grained EEG embeddings and coarse-grained classification results for semantic reconstruction and refinement.

Our contributions can be summarized as:

- We improve the self-supervised embedding method for EEG time-domain features, and introduce the frequency features to enhance EEG representations.
- We eliminate the reliance on additional large-scale datasets, reducing the data usage from 132k to 12k.
- BrainVis generates images with higher accuracy and better quality, and also overcomes previous limitation that was limited to only coarse-grained reconstruction.

The experimental results demonstrate that our proposed BrainVis outperforms the state-of-the-art (SOTA) in both semantic reconstruction and generation quality.

2 Related Works

2.1 Reconstructing Visual Stimuli from fMRI

Functional Magnetic Resonance Imaging (fMRI) boasts higher spatial resolution, better informative capacity and lower noise than EEG, facilitating its prevalence in visual reconstruction efforts (Du et al. 2022). Early studies (Kay et al. 2008; Wen et al. 2018; Güçlü and van Gerven 2015) leveraged linear regression alongside traditional or DL features for visual categorization or reconstruction through deep decoding networks (Belyi et al. 2019). With the advent of GANs (Goodfellow et al. 2014), a shift towards employing GANs for visual reconstruction has emerged (Shen et al. 2019; Fang, Qi, and Pan 2020).

Recently, a study (Lin, Sprague, and Singh 2022) used pre-trained CLIP model (Radford et al. 2021) to obtain embeddings of images and their artificial captions, aligning fMRI with these CLIP embeddings, then used it as the conditions for image generation by StyleGAN2. A study (Takagi and Nishimoto 2023a) transferred this latent embedding alignment to LDM (Rombach et al. 2022), achieving higher-quality reconstruction. Subsequently, works that centered around CLIP and LDM (Ozcelik and VanRullen 2023; Chen et al. 2023; Lu et al. 2023; Takagi and Nishimoto 2023b) continued to improve the accuracy and image quality of visual reconstructions, including introducing vector quantized-variational autoencoder (VQ-VAE) (Van Den Oord, Vinyals et al. 2017) and masked brain modeling (MBM) based on MAE (He et al. 2022) for better fMRI feature embedding. However, applying fMRI in practical settings is limited due to high cost, large data scale, and high processing complexity.

2.2 Reconstructing Visual Stimuli from EEG

EEG, by contrast, is more accessible and economically viable than fMRI. Nonetheless, its lower spatial precision and

inherent noise considerably complicate the reconstruction of visual stimuli. Early studies (Kavasidis et al. 2017) used LSTM for EEG classification and subsequently employed variational autoencoders (VAE) and GAN for image generation from EEG features, demonstrating the potential of EEG in conveying visual semantics. However, the feasibility of such attempts, constrained by EEG’s intrinsic limitations and the small size of EEG-Image pair datasets, remained limited under frameworks utilizing GAN (Tirupattur et al. 2018; Singh et al. 2023).

Inspired by MBM (Chen et al. 2023), the recently proposed DreamDiffusion (Bai et al. 2023) embeds time-domain features of EEG using MAE and aligns them with CLIP-encoded images, as conditions of pre-trained LDM to achieve coarse-grained category reconstruction. However, it only captures the time-domain features of EEG signals, and the ability of its models’ unsupervised feature embedding relies on pre-training on an additional large-scale self-collected EEG dataset (approximately 120,000 samples), indicating that it requires further enhancement in the representation capability of EEG features. Moreover, the condition of well pre-trained stable diffusion is text embedding, but DreamDiffusion directly aligns EEG features with image embeddings in CLIP space, which may introduce additional semantic noise, since text and image embeddings are not entirely equivalent.

3 Method

3.1 Preliminary

CLIP (Radford et al. 2021) is a pre-trained model for image-text similarity measurement, which embeds them in the same latent space with the contrastive learning. It mainly consists of an image encoder and a text encoder.

Stable diffusion (Rombach et al. 2022) is a text-to-image generation model, which uses CLIP embedding of text as its conditional input. It guides the denoising process from random noise by controlling the conditional input of the U-Net, realizing the generation of images with specified semantics.

BLIP-2 (Li et al. 2022) is a visual-language pre-trained model that can generate captions from images. It utilizes pre-trained image and language models with fixed parameters, and uses a query transformer to fill the gap between their modalities.

3.2 Overview

In Figure 2, we present BrainVis, which comprises three components: EEG encoder, semantic interpolation cross-modal alignment module, and cascaded diffusion models. The EEG encoder leverages self-supervised latent masked modeling to extract time-domain features and uses LSTM with Fast Fourier Transform (FFT) for frequency-domain features. The time and frequency branches are fine-tuned jointly with a visual semantic classifier to obtain time-frequency embeddings. These embeddings are then aligned with the semantic interpolation of CLIP embeddings, which represent visual stimuli labels and fine-grained captions generated by BLIP-2 (Li et al. 2022). Finally, cascaded diffusion models utilize the aligned embeddings for semantic reconstruction and the classification results for semantic refinement.

3.4 Semantic Interpolation Cross-modal Alignment

To achieve high-quality image reconstruction, we use a pre-trained stable diffusion (Rombach et al. 2022) model as the backbone generator. Previous work (Bai et al. 2023) aligned EEG embeddings with image CLIP embeddings before inputting them to the stable diffusion (SD) model. However, SD requires textual descriptions as input, and due to the gap between image and text CLIP embeddings (Zhou et al. 2022), they failed to reconstruct fine-grained semantic. To adapt SD for our task, we align EEG signal embeddings with text semantic embeddings.

For each instance, we only have coarse category annotations like “cat” and its CLIP embeddings c_{label} , which does not capture the complex semantics in the image. To incorporate more fine-grained semantics, we generate pseudo captions using BLIP-2 (Li et al. 2022). We then obtain the CLIP embeddings of the captions c_{cap} through CLIP encoder. However, aligning EEG features with c_{cap} is challenging. To address this, we align EEG features with the interpolation of fine and coarse-grained semantics, represented by generated captions and category annotations, respectively. The semantic interpolation aims to blend coarse and fine-grained semantics smoothly, and c_{label} highlights the primary semantic components of c_{cap} to ease the alignment difficulty.

We use a network composed of fully connected layers with residual connections to achieve this. Technically, we maximize the cosine similarity between the output of the alignment network c_{EEG} and c_{label} and c_{cap} . The loss function L_{si} for semantic interpolation alignment is defined as:

$$L_{si} = 2 - \frac{c_{cap} \cdot c_{EEG}}{|c_{cap}| |c_{EEG}|} - \frac{c_{label} \cdot c_{EEG}}{|c_{label}| |c_{EEG}|} \quad (4)$$

3.5 Cascaded Diffusion Models

Due to the inevitable imperfect alignment, there exist information loss and semantic noise in our reconstruction process. To mitigate the negative impact, we propose cascaded diffusion models. We adopt different levels of semantics as conditional inputs for the pre-trained stable diffusion (Rombach et al. 2022) model to guide the image reconstruction process.

First, we use c_{EEG} as condition, performing reverse diffusion in the latent space to reconstruct the semantics images. However, the reconstructed images are of low quality due to semantic noise and information loss in c_{EEG} . Therefore, we refine the incomplete denoised latents from reverse diffusion process by using unambiguous EEG classification labels as the new condition, which are from Sec.3.3. It reduces the semantic noises and yields higher-quality results.

4 Experiments

4.1 Dataset and implementation

Dataset. Our experimental setup employs an EEG-image pairs dataset named Block-Design Visually-Evoked (BDVE) (Spampinato et al. 2017; Palazzo et al. 2020a,b), encompassing 11,466 EEG sequences recorded from 128-channel electrodes, filtered through a 5-95 Hz filter. These

sequences were associated with 40 image classes. To elicit neural responses, six subjects were presented with a total of 2000 object images. These visual stimuli were selected from a subset of the widely used ImageNet (Russakovsky et al. 2015) dataset and comprised 40 classes, each containing 50 easily recognizable images. To ensure the exclusion of potential interference from previously shown images, the first 40 ms of each recorded EEG sequence were discarded, and the following 440 ms of EEG data were utilized for the experiments. We follow the official (Spampinato et al. 2017; Palazzo et al. 2020a) and baselines (Kavasidis et al. 2017; Bai et al. 2023), split the dataset into training, validation, and testing sets using an 8:1:1 ratio based on images instead of subjects, avoiding semantic overlap.

Implementation details. We follow the optimal parameter settings of prior works (Chen et al. 2023; Bai et al. 2023) and empirically set our parameters in Section 3: $c = 128$, $l = 440$, $n = 110$, $d = 1024$, $r_M = 0.75$ and $n_t = 660$. Moreover, the pre-trained stable diffusion model is v1-5-pruned-emaonly, while the pre-trained CLIP encoder is ViT-L/14. Transformer for visible feature extraction consists of 8 self-attention blocks, and for latent masked reconstruction comprises 4 cross-attention blocks. In each block, the attention heads are set to 16, and feed-forward network dimension is fixed at 4096. Additionally, the size of LSTM is 128. We employ a learning rate of 0.001 with a batch size of 128. Pre-training epochs are 300 for time encoder and 900 epochs for frequency encoder. Fine-tuning for time encoder lasts 80 epochs, and joint fine-tuning for time and frequency encoder lasts 30 epochs. Cross-modal EEG alignment fine-tuning is performed for 200 epochs.

4.2 Evaluation metrics

EEG Classification Accuracy (CA). CA measures the accuracy of EEG classification. It reflects the extent to which EEG’s latent features are correlated with coarse-grained visual semantics.

N -way Top- K Classification Accuracy of Generation (GA). Following (Chen et al. 2023; Bai et al. 2023), we utilize N -way Top- K accuracy to evaluate the semantic correctness of the reconstruction results. For multiple trials, the top- K and classification accuracies are calculated based on $N - 1$ randomly selected classes, along with the correct class. Both the ground-truth and generated images are initially inputted into a pre-trained ImageNet1K classifier (Dosovitskiy et al. 2020). We then examine whether the top- K classification among the N selected classes matched the ground-truth classification. In our case, we set $N = 50$ and $K = 1$.

Inception Score (IS). IS is employed to evaluate the diversity of the reconstructed images, providing insights into their quality. For a detailed definition, please refer to (Salimans et al. 2016).

Structural Similarity Index Measure (SSIM). SSIM quantifies the similarity between images based on brightness, contrast, and structure. It is a low-level measure of image quality.

F1-Score. F1-Score is the harmonic mean of precision and recall, used to measure EEG classification performance.



Figure 4: Comparison of reconstructed images' quality.



Figure 5: Comparison of reconstructed images with DreamDiffusion on the same ground truth (GT) image.

Methods	Subject	GA \uparrow	IS \uparrow	FID \downarrow
DreamDiffusion	4	0.4580	-	-
BrainVis (Ours)	4	0.4927	31.5281	121.0212
Brain2Image	Average	-	5.0700	-
NeuroVision		-	5.1500	-
DCLS-GAN		-	6.6400	-
ESG-ADA		-	10.8200	174.1300
MB2C		-	12.8500	153.3700
BrainVis (Ours)	Average	0.4546	30.9985	126.6576

Table 1: Comparison with image reconstruction baselines. '-' are not publicly available.

4.3 Comparison against other methods

Our comparative experiments include image reconstruction and EEG classification. The baselines of image reconstructions include DreamDiffusion (Bai et al. 2023), Brain2Image (Kavassidis et al. 2017), NeuroVision (Khare et al. 2022), DCLS-GAN (Fares, Zhong, and Jiang 2020), ESG-ADA (Singh et al. 2024) and MB2C (Wei et al. 2024). Notably, DreamDiffusion only reports GA on subject 4. The baselines of EEG classification include EEG-CN (Palazzo et al. 2020a), Brain2Image (Kavassidis et al. 2017), S-EEGNet (Shimizu and Srinivasan 2022) and KD-STFT (Ferrante et al. 2024). Furthermore, since we aim to reconstruct semantics, low-level metrics are not considered.

Quantitative results. To compare image reconstruction capabilities, we conduct experiments generating and evaluating

Method	Top-1 CA \uparrow	Top-3 CA \uparrow	Top-5 CA \uparrow	F1-Score \uparrow
EEG-CN	0.3130	-	-	-
Brain2Image	0.1648	0.3790	0.5524	0.1607
S-EEGNet	0.2520	-	-	-
KD-STFT	0.4120	0.7530	0.8782	0.4027
BrainVis (Ours)	0.4766	0.7923	0.9120	0.4323

Table 2: Comparison with EEG classification baselines. '-' are not publicly available.

4 images per EEG sample for all subjects. For EEG representation capability, we conduct EEG classification experiments.

The results in Table 1 show that BrainVis surpasses the existing SOTA by 7.04%, 186.49%, and 27.26% in GA, IS, and FID, respectively. It demonstrates that BrainVis has the best reconstruction semantic fidelity and generation quality.

The results in Table 2 show that BrainVis surpasses the existing SOTA by 15.68%, 5.22%, 3.85%, and 7.35% in Top-1, Top-3, Top-5 CA, and F1-Score, respectively. It demonstrates that our proposed EEG encoding (LMM+TFE) method has the best EEG representation capability.

Qualitative results. In Figure 4, we compare our reconstructed images for three categories (Airliner, Jack-o'-Lantern, and Panda) with classic GAN-based Brain2Image and diffusion-based DreamDiffusion, which is widely considered as the SOTA in image reconstruction quality. Our images show higher quality, highlighting our method's effectiveness.

In Figure 5, we compare our reconstructed images with DreamDiffusion using the same ground truth (GT) images.

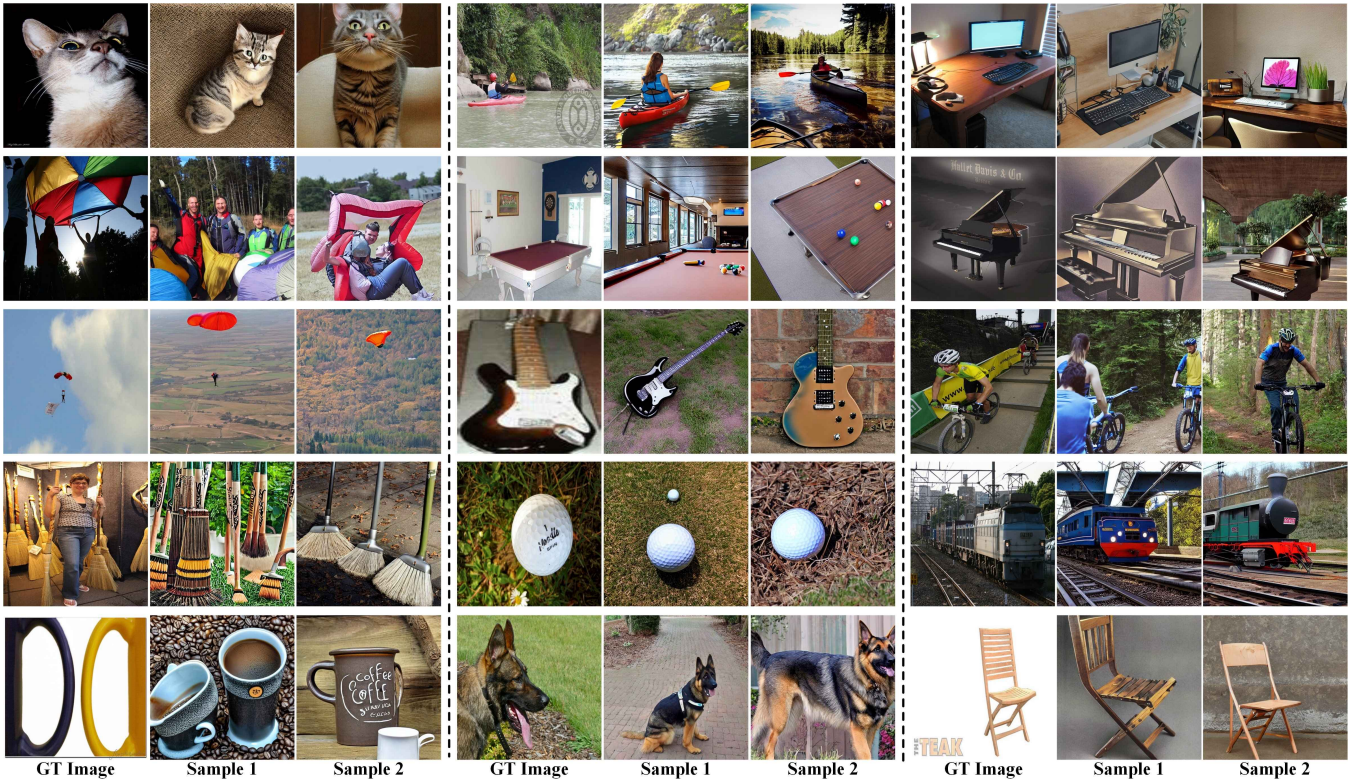


Figure 6: Image reconstruction results and the GT images. We not only reconstruct the correct types, but also capture the fine-grained semantics to some extent, such as prominent numerical, color, or behavioral features.

Models	Full	w/o TiB	w/o FrB	w/o PT	w/o FT
Top-1 CA \uparrow	0.4766	0.2943	0.4397	0.2783	0.2495

Table 3: Ablation analysis of components of EEG encoder. TiB, FrB, PT and FT respectively stand for time branch, frequency branch, LMM pre-training and TFE fine-tuning.

Due to the limited GTs publicly available from DreamDiffusion, only 3 images are available for comparison under consistent conditions. Among them, we correctly reconstruct the styles and colors of the car and chair, as well as the behavior and environment of the cat, while DreamDiffusion failed.

4.4 Ablation Study

Components of EEG encoder. In Table 3, we conducted an ablation study through classification experiments to analyze the impact of the main components in the EEG encoder on EEG representation. The results show that time-domain features, frequency-domain features, LMM pre-training and time-frequency embedding positively affect performance.

The impact of time branch, frequency branch and cascaded models on image reconstruction. The results in Table 4 show that time-domain features dominate image reconstruction, while frequency-domain features improve it. Additionally, each stage of the cascaded diffusion models positively contributes to the reconstruction process.

Models		GA \uparrow	IS \uparrow	FID \downarrow
w/o FrB	w/o Refinement	0.1218	16.5092	255.3962
	w/o Semantic	0.4147	28.1505	137.8096
	Cascaded	0.4202	29.5453	132.8096
w/o TiB	w/o Refinement	0.1291	17.4441	244.2778
	w/o Semantic	0.2782	28.5453	129.0044
	Cascaded	0.2876	30.3657	127.6774
Full	w/o Refinement	0.1307	17.8735	242.9537
	w/o Semantic	0.4501	28.8167	129.1161
	Cascaded	0.4546	30.9985	126.6576

Table 4: Ablation study on the time branch, frequency branch and cascaded models on image reconstruction.

Pre-trained with	CA \uparrow	GA \uparrow	IS \uparrow	FID \downarrow
BDVE (Ours, 12k)	0.4766	0.4546	30.9985	126.6576
MOABB (120k)	0.3413	0.3127	29.0601	147.1737
BDVE+MOABB	0.4739	0.4523	30.5221	126.7201
None	0.2783	0.2386	29.1481	145.7066

Table 5: Ablation study on pre-training data.

n_t	None	220	330	660	990
Top-1 CA \uparrow	0.4118	0.4382	0.4326	0.4397	0.3597

Table 6: Ablation study on codewords number n_t on CA (w/o the frequency branch).

Model	Time (s/epoch) ↓	Params ↓	Top-1 CA ↑
CNN	75.7974	5.1410M	0.2537
LSTM	13.5687	0.1538M	0.2578

Table 7: Comparison of training time, parameter numbers and CA between different frequency encoder backbones.

Pre-training data. Previous work used various datasets from MOABB (Jayaram and Barachant 2018), including many EEG recordings unrelated to visual tasks. The number of EEG channels and their meaning vary, and EEGs with fewer than 128 channels are unscientifically filled by self-replication. Table 5 shows that including these data in our pre-training may even slightly negatively impact performance.

Optimization of codewords number. In Table 6, we present the results of ablation analysis on the total number of codewords n_t . Based on the results, we set $n_t = 660$.

Backbone of frequency branch. We observe that using complex networks in the frequency branch precipitates rapid overfitting. To mitigate this, we favor simpler backbones for the frequency branch, such as convolutional neural network (CNN) and LSTM, which are commonly used to process EEG. We choose the CNN proposed in (Spampinato et al. 2017) as an example. The results in Table 7 show that using LSTM effectively reduces training costs and slightly improves performance.

4.5 Image Reconstruction Results

In Figure 6, we present part of the reconstructed results. We can reconstruct the correct coarse-grained categories and preserve fine-grained details. For example, considering the first column, we successfully reconstruct a cat looking up, parachutes on the ground or in the air, and the quantitative relationship between brooms/cups and their GT images, etc.

4.6 Discussion

In figure 7, we present part of the reconstruction results under incorrect coarse-grained classification. Although the generated object is incorrect, there are noticeable resemblances between these generated samples and real images, particularly in terms of color, shape or surface textures/materials. This observation implies that the visual information encoded in human EEG signals may prioritize fundamental properties of objects rather than specific object categories. The classification of visual stimuli from EEG signals involves decoding and categorizing information pertaining to color, shape and various other features. Building upon this hypothesis, decoding individual properties of visual information, such as color and shape in isolation may offer an effective avenue for EEG analysis and visual reconstruction.

5 Conclusion

This paper proposes BrainVis, a novel pipeline for EEG-based image reconstruction. BrainVis uses self-supervised latent masked modeling and LSTM to embed EEG as time-frequency features, which are then aligned with semanti-

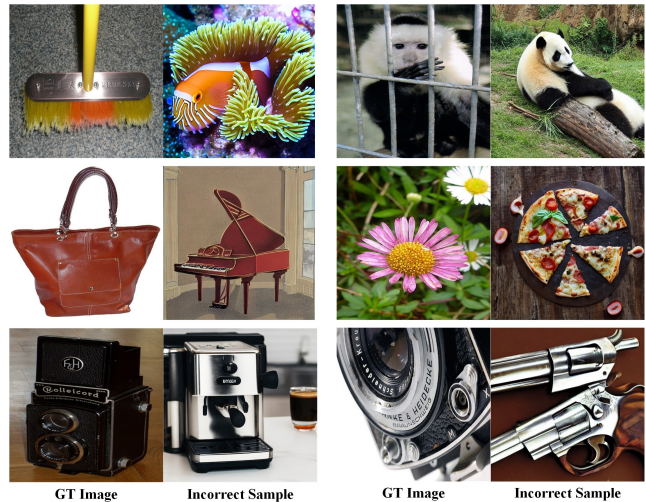


Figure 7: Examples of incorrect reconstruction results.

cally interpolated CLIP embeddings. The aligned results and predicted category embeddings serve as conditions for cascaded diffusion models for image reconstruction. BrainVis surpasses the SOTA in EEG representation, semantic reconstruction and generation quality, eliminates the need for additional unrelated data, and overcomes the previous limitation of being unable to reconstruct fine-grained semantics.

References

- Al-Fahoum, A. S.; and Al-Fraihat, A. A. 2014. Methods of EEG signal features extraction using linear analysis in frequency and time-frequency domains. *International Scholarly Research Notices*, 2014.
- Alzahab, N. A.; Apollonio, L.; Di Iorio, A.; Alshalak, M.; Iarlori, S.; Ferracuti, F.; Monteriù, A.; and Porcaro, C. 2021. Hybrid deep learning (hDL)-based brain-computer interface (BCI) systems: a systematic review. *Brain sciences*, 11(1): 75.
- Bai, Y.; Wang, X.; Cao, Y.; Ge, Y.; Yuan, C.; and Shan, Y. 2023. DreamDiffusion: Generating High-Quality Images from Brain EEG Signals. *arXiv preprint arXiv:2306.16934*.
- Banaszkiewicz, A.; Matuszewski, J.; Szczepanik, M.; Kosowski, B.; Mostowski, P.; Rutkowski, P.; Śliwińska, M.; Jednoróg, K.; Emmorey, K.; Marchewka, A.; et al. 2021. The role of the superior parietal lobule in lexical processing of sign language: Insights from fMRI and TMS. *Cortex*, 135: 240–254.
- Beliy, R.; Gaziv, G.; Hoogi, A.; Strappini, F.; Golan, T.; and Irani, M. 2019. From voxels to pixels and back: Self-supervision in natural-image reconstruction from fMRI. *Advances in Neural Information Processing Systems*, 32.
- Chen, Z.; Qing, J.; Xiang, T.; Yue, W. L.; and Zhou, J. H. 2023. Seeing beyond the brain: Conditional diffusion model with sparse masked modeling for vision decoding. In *Proceedings of the IEEE/CVF Conference on Computer Vision and Pattern Recognition*, 22710–22720.

- Cheng, M.; Liu, Q.; Liu, Z.; Zhang, H.; Zhang, R.; and Chen, E. 2023. TimeMAE: Self-Supervised Representations of Time Series with Decoupled Masked Autoencoders. *arXiv preprint arXiv:2303.00320*.
- Dosovitskiy, A.; Beyer, L.; Kolesnikov, A.; Weissenborn, D.; Zhai, X.; Unterthiner, T.; Dehghani, M.; Minderer, M.; Heigold, G.; Gelly, S.; et al. 2020. An image is worth 16x16 words: Transformers for image recognition at scale.
- Du, B.; Cheng, X.; Duan, Y.; and Ning, H. 2022. fmri brain decoding and its applications in brain-computer interface: A survey. *Brain Sciences*, 12(2): 228.
- Fang, T.; Qi, Y.; and Pan, G. 2020. Reconstructing perceptive images from brain activity by shape-semantic gan. *Advances in Neural Information Processing Systems*, 33: 13038–13048.
- Fares, A.; Zhong, S.-h.; and Jiang, J. 2020. Brain-media: A dual conditioned and lateralization supported gan (dcls-gan) towards visualization of image-evoked brain activities. In *Proceedings of the 28th ACM International Conference on Multimedia*, 1764–1772.
- Ferrante, M.; Boccato, T.; Bargione, S.; and Toschi, N. 2024. Decoding EEG signals of visual brain representations with a CLIP based knowledge distillation. In *ICLR 2024 Workshop on Learning from Time Series For Health*.
- Geirnaert, S.; Vandecappelle, S.; Alickovic, E.; de Cheveigne, A.; Lalor, E.; Meyer, B. T.; Miran, S.; Francart, T.; and Bertrand, A. 2021. Electroencephalography-based auditory attention decoding: Toward neurosteered hearing devices. *IEEE Signal Processing Magazine*, 38(4): 89–102.
- Goodfellow, I.; Pouget-Abadie, J.; Mirza, M.; Xu, B.; Warde-Farley, D.; Ozair, S.; Courville, A.; and Bengio, Y. 2014. Generative adversarial nets. *Advances in neural information processing systems*, 27.
- Güçlü, U.; and van Gerven, M. A. 2015. Deep neural networks reveal a gradient in the complexity of neural representations across the ventral stream. *Journal of Neuroscience*, 35(27): 10005–10014.
- He, K.; Chen, X.; Xie, S.; Li, Y.; Dollár, P.; and Girshick, R. 2022. Masked autoencoders are scalable vision learners. In *Proceedings of the IEEE/CVF conference on computer vision and pattern recognition*, 16000–16009.
- Hutmacher, F. 2019. Why is there so much more research on vision than on any other sensory modality? *Frontiers in psychology*, 10: 2246.
- Jayaram, V.; and Barachant, A. 2018. MOABB: trustworthy algorithm benchmarking for BCIs. *Journal of neural engineering*, 15(6): 066011.
- Kavassidis, I.; Palazzo, S.; Spampinato, C.; Giordano, D.; and Shah, M. 2017. Brain2image: Converting brain signals into images. In *Proceedings of the 25th ACM international conference on Multimedia*, 1809–1817.
- Kay, K. N.; Naselaris, T.; Prenger, R. J.; and Gallant, J. L. 2008. Identifying natural images from human brain activity. *Nature*, 452(7185): 352–355.
- Khare, S.; Choubey, R. N.; Amar, L.; and Udutalapalli, V. 2022. Neurovision: perceived image regeneration using cprogan. *Neural Computing and Applications*, 34(8): 5979–5991.
- Khosla, A.; Khandnor, P.; and Chand, T. 2020. A comparative analysis of signal processing and classification methods for different applications based on EEG signals. *Biocybernetics and Biomedical Engineering*, 40(2): 649–690.
- Lai, C. Q.; Ibrahim, H.; Abdullah, M. Z.; Abdullah, J. M.; Suandi, S. A.; and Azman, A. 2018. Artifacts and noise removal for electroencephalogram (EEG): A literature review. In *2018 IEEE Symposium on Computer Applications & Industrial Electronics (ISCAIE)*, 326–332. IEEE.
- Lee, Y.-E.; Lee, S.-H.; Kim, S.-H.; and Lee, S.-W. 2023. Towards voice reconstruction from EEG during imagined speech. *arXiv preprint arXiv:2301.07173*.
- Li, J.; Li, D.; Xiong, C.; and Hoi, S. 2022. Blip: Bootstrapping language-image pre-training for unified vision-language understanding and generation. In *International Conference on Machine Learning*, 12888–12900. PMLR.
- Lin, S.; Sprague, T.; and Singh, A. K. 2022. Mind reader: Reconstructing complex images from brain activities. *Advances in Neural Information Processing Systems*, 35: 29624–29636.
- Lu, Y.; Du, C.; Wang, D.; and He, H. 2023. MindDiffuser: Controlled Image Reconstruction from Human Brain Activity with Semantic and Structural Diffusion. *arXiv preprint arXiv:2303.14139*.
- Ozcelik, F.; and VanRullen, R. 2023. Natural scene reconstruction from fMRI signals using generative latent diffusion. *Scientific Reports*, 13(1): 15666.
- Palazzo, S.; Spampinato, C.; Kavassidis, I.; Giordano, D.; Schmidt, J.; and Shah, M. 2020a. Decoding brain representations by multimodal learning of neural activity and visual features. *IEEE Transactions on Pattern Analysis and Machine Intelligence*, 43(11): 3833–3849.
- Palazzo, S.; Spampinato, C.; Schmidt, J.; Kavassidis, I.; Giordano, D.; and Shah, M. 2020b. Correct block-design experiments mitigate temporal correlation bias in EEG classification. *arXiv preprint arXiv:2012.03849*.
- Radford, A.; Kim, J. W.; Hallacy, C.; Ramesh, A.; Goh, G.; Agarwal, S.; Sastry, G.; Askell, A.; Mishkin, P.; Clark, J.; et al. 2021. Learning transferable visual models from natural language supervision. In *International conference on machine learning*, 8748–8763. PMLR.
- Rombach, R.; Blattmann, A.; Lorenz, D.; Esser, P.; and Ommer, B. 2022. High-resolution image synthesis with latent diffusion models. In *Proceedings of the IEEE/CVF conference on computer vision and pattern recognition*, 10684–10695.
- Russakovsky, O.; Deng, J.; Su, H.; Krause, J.; Satheesh, S.; Ma, S.; Huang, Z.; Karpathy, A.; Khosla, A.; Bernstein, M.; et al. 2015. Imagenet large scale visual recognition challenge. volume 115, 211–252. Springer.
- Salimans, T.; Goodfellow, I.; Zaremba, W.; Cheung, V.; Radford, A.; and Chen, X. 2016. Improved techniques for training gans. volume 29.
- Shen, G.; Horikawa, T.; Majima, K.; and Kamitani, Y. 2019. Deep image reconstruction from human brain activity. *PLoS computational biology*, 15(1): e1006633.
- Shimizu, H.; and Srinivasan, R. 2022. Improving classification and reconstruction of imagined images from EEG signals. *Plos one*, 17(9): e0274847.

Singh, P.; Dalal, D.; Vashishtha, G.; Miyapuram, K.; and Raman, S. 2024. Learning Robust Deep Visual Representations from EEG Brain Recordings. In *Proceedings of the IEEE/CVF Winter Conference on Applications of Computer Vision*, 7553–7562.

Singh, P.; Pandey, P.; Miyapuram, K.; and Raman, S. 2023. EEG2IMAGE: Image reconstruction from EEG brain signals. In *ICASSP 2023-2023 IEEE International Conference on Acoustics, Speech and Signal Processing (ICASSP)*, 1–5. IEEE.

Spampinato, C.; Palazzo, S.; Kavasidis, I.; Giordano, D.; Souly, N.; and Shah, M. 2017. Deep learning human mind for automated visual classification. In *Proceedings of the IEEE conference on computer vision and pattern recognition*, 6809–6817.

Takagi, Y.; and Nishimoto, S. 2023a. High-resolution image reconstruction with latent diffusion models from human brain activity. In *Proceedings of the IEEE/CVF Conference on Computer Vision and Pattern Recognition*, 14453–14463.

Takagi, Y.; and Nishimoto, S. 2023b. Improving visual image reconstruction from human brain activity using latent diffusion models via multiple decoded inputs. *arXiv preprint arXiv:2306.11536*.

Tirupattur, P.; Rawat, Y. S.; Spampinato, C.; and Shah, M. 2018. Thoughtviz: Visualizing human thoughts using generative adversarial network. In *Proceedings of the 26th ACM international conference on Multimedia*, 950–958.

Van Den Oord, A.; Vinyals, O.; et al. 2017. Neural discrete representation learning. *Advances in neural information processing systems*, 30.

Wei, Y.; Cao, L.; Li, H.; and Dong, Y. 2024. MB2C: Multi-modal Bidirectional Cycle Consistency for Learning Robust Visual Neural Representations. In *ACM Multimedia 2024*.

Wen, H.; Shi, J.; Zhang, Y.; Lu, K.-H.; Cao, J.; and Liu, Z. 2018. Neural encoding and decoding with deep learning for dynamic natural vision. *Cerebral cortex*, 28(12): 4136–4160.

Wu, M.; Teng, W.; Fan, C.; Pei, S.; Li, P.; and Lv, Z. 2023. An investigation of olfactory-enhanced video on eeg-based emotion recognition. *IEEE Transactions on Neural Systems and Rehabilitation Engineering*, 31: 1602–1613.

Zhou, Y.; Zhang, R.; Chen, C.; Li, C.; Tensmeyer, C.; Yu, T.; Gu, J.; Xu, J.; and Sun, T. 2022. Towards language-free training for text-to-image generation. In *Proceedings of the IEEE/CVF Conference on Computer Vision and Pattern Recognition*, 17907–17917.